An Empirical Low-Frequency Forecast Model Incorporating Diabatic Forcing

Christopher R. Winkler, Matthew Newman, and Prashant D. Sardeshmukh
NOAA-CIRES Climate Diagnostics Center, Boulder, Colorado

1. Introduction

The processes responsible for the evolution and maintenance of atmospheric low-frequency variability (LFV) have long been of interest in the meteorological community. Early efforts suggested barotropic instabilities of the zonally and meridionally varying basic state are essential to LFV (Simmons et al. 1983). Recent studies, however, have shown that LFV strongly depends on the spatial structure of anomalous time-varying external forcing (Sardeshmukh et al. 1997, Newman et al. 1997). This study is an attempt to clarify the role one forcing, tropical diabatic heating, has on LFV.

We consider the evolution of low-frequency eddies as

$$\frac{d\mathbf{x}}{dt} = \mathbf{L}\mathbf{x} + \mathbf{n} \qquad (1)$$

where $\mathbf{x}$ is some state variable suitably filtered, $\mathbf{L}$ is a linear dynamical operator, and $\mathbf{n}$ represents the combined effects of nonlinearities and external forcing on $\mathbf{x}$. Many previous investigators have specified $\mathbf{L}$ as a linearized version of the governing equations, parameterized $\mathbf{n}$ (usually setting $\mathbf{n} = 0$), and compared numerical model results to observations. In contrast our approach is empirical. We use the linear inverse modeling method (Penland and Sardeshmukh 1995) and try to model (1) as

$$\frac{d\mathbf{x}}{dt} = \mathbf{B}\mathbf{x} + \mathbf{F}_s . \qquad (2)$$

The operator $\mathbf{B}$ contains all linear dynamics of the system, including the linearly parameterizable effects of synoptic eddy feedbacks and damping. The $\mathbf{F}_s$ term is Gaussian white noise which models processes that cannot be parameterized linearly in $\mathbf{x}$. This approximation assumes that nonlinearities act on time scales much faster than the low-frequencies of interest in (1).

Linear inverse modeling determines the dynamical operator $\mathbf{B}$ from the observed statistics of $\mathbf{x}$ as

$$\mathbf{B} = \tau_0^{-1} \ln \left\{ \langle \mathbf{x}(t+\tau_0)\mathbf{x}^{\mathbf{T}}(t) \rangle \langle \mathbf{x}(t)\mathbf{x}^{\mathbf{T}}(t) \rangle^{-1} \right\} (3)$$

where angle brackets denote a time average. Penland and Magorian (1993) show that if (2) is a good model of the low-frequency eddies, then the best forecast at lead time τ is

$$\mathbf{x}(t+\tau) = \exp(\mathbf{B}\tau)\mathbf{x}(t) = \mathbf{G}(\tau)\mathbf{x}(t). \qquad (4)$$

Forecasts of $\mathbf{x}(t+\tau)$ differ from the true state because noise is present in (2). Nonetheless, if (2) reasonably describes LFV then forecasts using (4) will be good. Also, the statistics of $\mathbf{x}$ will be Gaussian and $\mathbf{B}$ will be independent of τ_0 (Penland and Sardeshmukh 1995).

Our state variable is defined as

$$\mathbf{x} = \begin{bmatrix} \psi_{750} \\ \psi_{250} \\ \mathbf{H} \end{bmatrix} \qquad (5)$$

Here ψ refers to streamfunction and $\mathbf{H}$ to tropical diabatic heating. By modeling $\mathbf{H}$ explicitly we can diagnose the temporal and spatial features of tropical heating significant for LFV, provided that (2) adequately describes the evolution of low-frequency anomalies. If $\mathbf{x}$ contained streamfunction alone (2) might still describe the system, but an analysis of the importance of diabatic heating relative to other processes in LFV (e.g. non-modal growth) could not be undertaken. We also find that defining $\mathbf{x}$ as in (5) produces better streamfunction forecasts than if $\mathbf{x}$ is defined only in terms of streamfunction.

2. Data and methodology

We have used 29 years (1969-70 to 1997-98) of DJF data in this study. The streamfunction fields are measured at 750 and 250 hPa in (5) and have been restricted to just the Northern Hemisphere (NH). The diabatic heating field is integrated from surface to tropopause and is taken from 30S-30N. The streamfunction and diabatic heating are dynamically consistent fields, that is the large-scale mass and vorticity balances are satisfied, as determined from the generalized baroclinic chi problem correction to NCEP Reanalysis winds (Sardeshmukh et al. 1999). All calculations were performed with data truncated to T12 though additional calculations using T21 fields show similar results. All variables have had the first 3 harmonics of their seasonal cycles removed and are filtered with a 7-day running mean to emphasize low frequencies. The streamfunction is then projected onto its leading 25 EOFs (~85% of the running mean variance), and the heating onto its first 5 EOFs (~30% of the running mean variance).
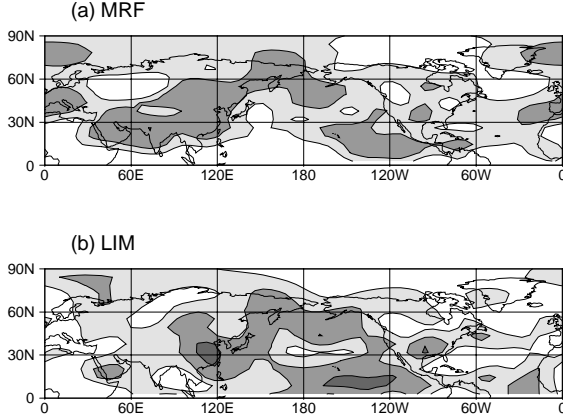
(a) MRF

(b) LIM

FIG. 1. Local anomaly correlations of week 2 250 hPa streamfunction forecasts for DJF 1996/7 and 1997/8 from (a) the MRF ensemble mean and (b) the linear inverse model. Contour interval is 0.2 and only contours greater than 0.4 are shown.
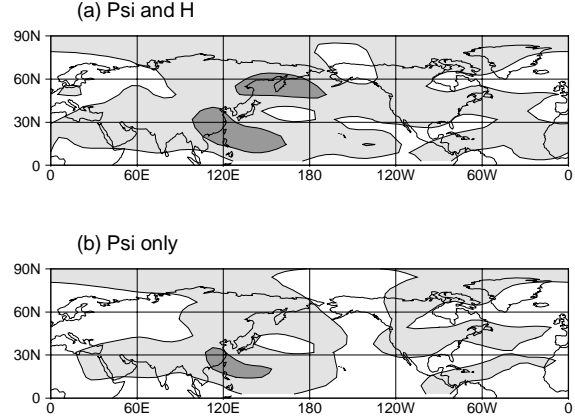

(a) Psi and H

(b) Psi only

FIG. 2. (a) Local anomaly correlations of week 2 LIM forecasts of 250 hPa for all winters. Contour interval is 0.2 and only contours greater than 0.4 are shown. (b) As in (a) but with $\mathbf{H} = 0$ for $\mathbf{x}(t)$ in (4).

Our method and analysis closely follows Penland and Sardeshmukh (1995). A jack-knifing procedure has been used to derive estimates of $\mathbf{B}$. In this procedure we sub-sample our data record by removing one of the available years, solve for $\mathbf{B}$ using a τ_0 of 7 days, and then generate forecasts in the independent year for any lead time τ. If the dynamics are truly linear $\mathbf{B}$ should not depend on the lag τ_0 on which it was trained. Moreover, if the statistics of $\mathbf{x}$ are stationary, then the normal modes of $\mathbf{B}$ should be stable and the only means for growth is through non-modal interaction. Both of these criteria are met by our model.

3. Validity of the model

Having obtained estimates of $\mathbf{B}$, we generated forecasts of $\mathbf{x}$ and compared the local anomaly correlations of our forecasts to several other simple models: climatology, persistence, and AR-1. In all cases the linear inverse model (LIM) forecasts yielded correlations significantly higher than the other models.

A more demanding test of the inverse model, however, is to compare forecast performance to a state-of-the-art numerical model. Figure 1 compares the skill of LIM forecasts and MRF ensemble mean forecasts of 250 hPa streamfunction at week 2 for two winters. South of 30N the LIM forecasts produce local anomaly correlations much higher than the MRF, particularly in the Pacific where correlations can be greater than 0.8. LIM correlations are also higher than the MRF in the North Pacific and over North America, but MRF correlations are higher than LIM correlations over Europe and central Asia. Figure 2a shows the local anomaly correlations of our model for all winters. The skill for the full period is

not as great as it is during the two winters for which we can compare with the MRF, but anomaly correlations are still greater than 0.4 over most of the hemisphere.

High skill in LIM forecasts relative to the MRF, as well as generally high anomaly correlations in all winters, gives us confidence in (2) as a model of low-frequency variability. Regions in which LIM forecasts are poor may indicate areas where nonlinearities, noise, or variables not present in our definition of $\mathbf{x}$ are important.

4. Importance of diabatic heating

Figure 2b shows the local anomaly correlations of LIM forecasts $\mathbf{x}(t + \tau)$ when tropical heating anomalies are

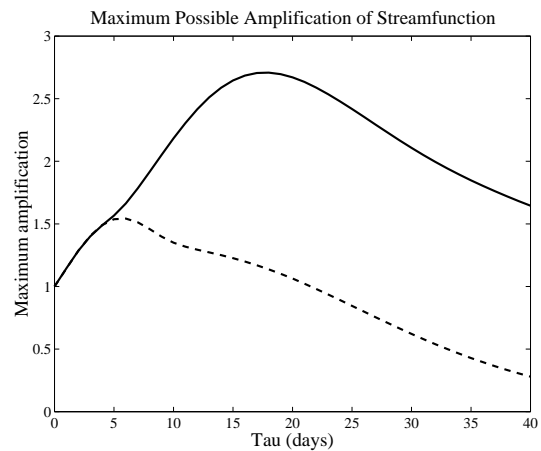Maximum Possible Amplification of Streamfunction

FIG. 3. Solid curve: the maximum amplification curve. Dashed curve: maximum possible amplification when generation of streamfunction by heating is eliminated in $\mathbf{G}(\tau)$.
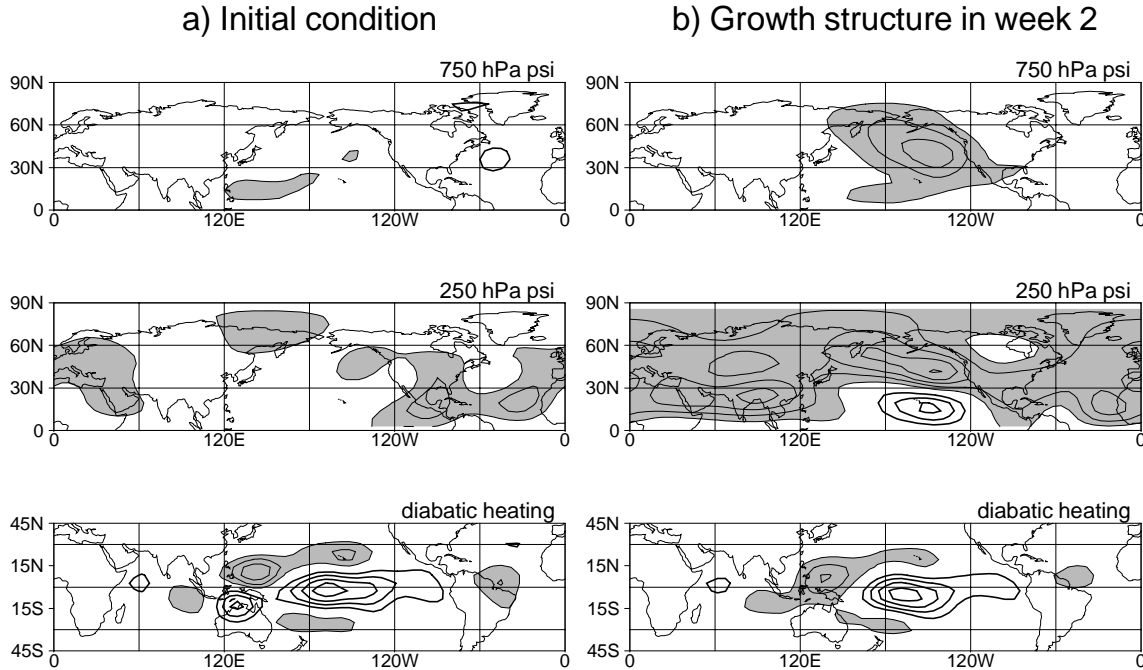
a) Initial condition

750 hPa psi

250 hPa psi

diabatic heating

b) Growth structure in week 2

750 hPa psi

250 hPa psi

diabatic heating

FIG. 4. (a) Initial condition of **x** that maximizes the growth of streamfunction anomalies at week 2. (b) Structure which the initial condition grows into eleven days later. Top two panels are 750 hPa streamfunction, middle two are 250 hPa streamfunction, and bottom two are tropical diabatic heating. Contour interval is arbitrary but the same between the left and right panels. Positive values are indicated by thick lines. Negative values are shaded.

eliminated from $\mathbf{x}(t)$ in (4). Clearly model skill is reduced over much of the hemisphere, particularly east of the dateline, indicating the importance of tropical heating.

The eigenanalysis of

$$\mathbf{G}(\tau)^{\mathbf{T}}\mathbf{D}\mathbf{G}(\tau) \qquad (6)$$

where **D** is a norm which maximizes the growth of streamfunction anomalies has been performed. The eigenanalysis reveals structures which optimally grow at some τ and the amplitude of that growth. A plot of the maximum growth as a function of τ (Fig. 3) peaks at 18 days. When the generation of streamfunction anomalies by tropical heating is turned off in $\mathbf{G}(\tau)$ (dashed curve in Fig. 3), streamfunction growth maximizes around 5 days and no growth is possible beyond 20 days. The maximum amplification curves thus show the crucial role of tropical diabatic heating for the growth of anomalies at week 2 and beyond.

The optimal initial conditions and evolved structures for maximum growth at week 2 are shown in Figure 4. The initial condition has little coherent information in the streamfunction but shows strong heating in the central Pacific and along the northwest coast of Australia. A

deep equivalent barotropic low off the Aleutians with evidence of wave propagation emanating from the central Pacific is seen in week 2 (Fig. 4b). The tropical heating pattern is relatively steady throughout the evolution, except over Australia. The significance of these structures for the actual growth of observed anomalies is verified in Figure 5. Shown is a scatterplot of the spatial
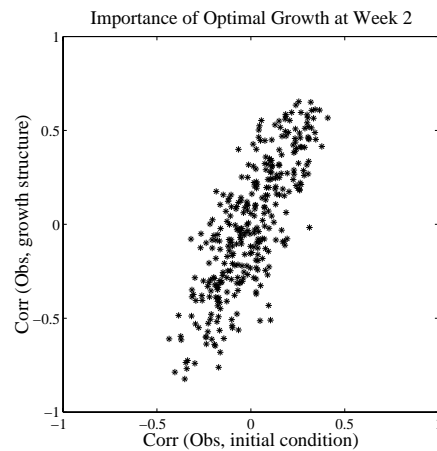
Importance of Optimal Growth at Week 2

FIG. 5. Scatterplot of the spatial correlation between observations and the pattern in Fig. 4b versus the spatial correlation of Fig. 4a and observations eleven days earlier. The strong positive slope indicates that optimal growth does occur in the system.

a) Initial condition
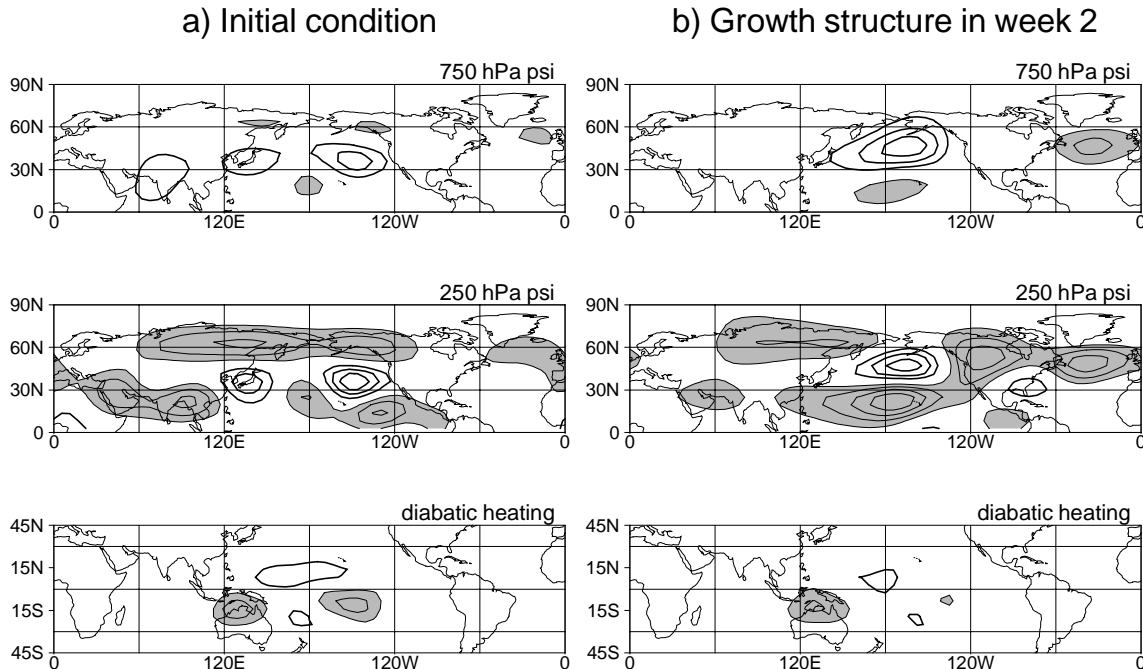

b) Growth structure in week 2

FIG. 6. As in Fig. 4, but for the second leading eigenstructures of (6).

correlation of observed low-frequency streamfunction anomalies with the top two panels of Fig. 4b against the spatial correlation of Fig. 4a with observations eleven days earlier. The high temporal correlation between projections on the patterns of Fig. 4 (R=0.79) indicates that this optimal structure is truly important in the development of low-frequency anomalies in the real atmosphere. Also, the relevance of optimal growth shown in Fig. 5 is further evidence that (2) is a good model of the anomalous low-frequency circulation.

Figure 6 shows the second leading structure for week 2 growth. All other structures decay by this time, while this structure weakly amplifies into a PNA pattern. Some initial cooling is present over Australia and the central Pacific with weaker heating north of the Equator. The streamfunction field for this structure has prominent anomalies tilted against the mean flow near the Asian jet. These initial patterns, in contrast to those for the leading structure, suggest that tropical forcing may be less important to the development of this PNA structure.

5. Summary and conclusions

We have shown that a linear inverse model of streamfunction and tropical diabatic heating can describe the low-frequency variability of Northern Hemisphere winter. Linear inverse model forecasts have higher skill than MRF ensemble mean forecasts in the tropics and comparable skill in the extratropics. Further analysis shows

that the structure and magnitude of tropical diabatic heating perturbations is critical for the long-term (> 10 day) evolution of low-frequency circulation anomalies. Indeed, figures 4 and 5 strongly indicate that the principal growth structure in the system is diabatically forced, though other structures may be less dependent on the tropical heating. We thus conclude that tropical diabatic heating is essential to the long-term development and maintenance of extratropical Northern Hemisphere wintertime low-frequency variability.

References

Newman, M., P. D. Sardeshmukh, and C. Penland, 1997: Stochastic forcing of the wintertime extratropical flow. *J. Atmos. Sci.*, **54**, 435-455.

Penland, C., and T. Magorian, 1993: Prediction of Niño-3 sea surface temperatures using linear inverse modeling. *J. Climate*, **6**, 1067-1076.

Penland, C., and P. D. Sardeshmukh, 1995: The optimal growth of tropical sea surface temperature anomalies. *J. Climate*, **8**, 1999-2023.

Sardeshmukh, P. D., M. Newman, and M. D. Borges,1997: Free barotropic Rossby wave dynamics of the wintertime low-frequency flow. *J. Atmos. Sci*, **54**, 5-23.

—, —, and C. R. Winkler, 1999: Dynamically consistent estimates of diabatic heating. Proceedings of the Twenty-fourth annual Climate Diagnostics and Prediction Workshop, Tucson, AZ.

Simmons, A. J., J. M. Wallace, and G. W. Branstator, 1983: Barotropic wave propagation and instability, and atmospheric teleconnection patterns. *J. Atmos. Sci.*, **40**, 1363-1392.